

NASA/TM-1998-206551



Determination of Sun Angles for Observations of Shock Waves on a Transport Aircraft

*David F. Fisher, Edward A. Haering, Jr., Gregory K. Noffz, and Juan I. Aguilar
Dryden Flight Research Center
Edwards, California*

National Aeronautics and
Space Administration

Dryden Flight Research Center
Edwards, California 93523-0273

September 1998

NOTICE

Use of trade names or names of manufacturers in this document does not constitute an official endorsement of such products or manufacturers, either expressed or implied, by the National Aeronautics and Space Administration.

Available from the following:

NASA Center for AeroSpace Information (CASI)
7121 Standard Drive
Hanover, MD 21076-1320
(301) 621-0390

National Technical Information Service (NTIS)
5285 Port Royal Road
Springfield, VA 22161-2171
(703) 487-4650

ABSTRACT

Wing compression shock shadowgraphs were observed on two flights during banked turns of an L-1011 aircraft at a Mach number of 0.85 and an altitude of 35,000 ft (10,700 m). Photos and video recording of the shadowgraphs were taken during the flights to document the shadowgraphs. Bright sunlight on the aircraft was required. The time of day, aircraft position, speed and attitudes were recorded to determine the sun azimuth and elevation relative to the wing quarter chordline when the shadowgraphs were visible. Sun elevation and azimuth angles were documented for which the wing compression shock shadowgraphs were visible. The shadowgraph was observed for high to low elevation angles relative to the wing, but for best results high sun angles relative to the wing are desired. The procedures and equations to determine the sun azimuth and elevation angle with respect to the quarter chordline is included in the Appendix.

INTRODUCTION

In the late 1940's, during high speed dives in single-engine fighter aircraft, pilots noticed a visible indication of the normal shock wave over the wing. One of the first to notice this was Major Fredrick A. Borsodi of the U.S. Army Air Force.[1] About this same time, when the National Advisory Committee for Aeronautics (NACA) was testing small airfoils in transonic flow on fighter aircraft, the pilot could watch the shock wave travel over the test airfoil, if the aircraft was in the right position relative to the sun. What these pilots were watching were natural shadowgraphs caused by the refraction of the sun rays passing through the density discontinuity of the shock. Today, airline passengers can often see the same phenomenon. The purpose of this paper is to document sun elevations and azimuth angles for which the wing compression shock shadowgraphs are visible. This paper will present several shock wave shadowgraphs observed on the wing of an L-1011 aircraft at $M = 0.85$ and an altitude of 35,000 ft (10,700 m) and will document the relative angles of the wing to the sun when this phenomenon is visible.

BACKGROUND

The shadowgraph is a simple technique, frequently used for visualizing the shock position on models in wind tunnels, shock tubes, and ballistic ranges.[2] This technique needs a bright source of parallel light rays. In flight, the sun serves this purpose. The flight shadowgraph method was first described by the report of Cooper and Rathert [1] in 1948 for straight wing airplanes. Other authors have discussed the flight technique briefly [2, 3, 4, and 5], but did not define the required sun angle to the wing. The explanation of the flight shadowgraph as described by Cooper and Rathert is shown in figure 1. The change in density of the air at the shock causes the light rays to be refracted. Because the pressure (and density) change is greater near the surface, the refraction is greater. This results in a dark band immediately behind the shock wave, followed by a light band. Cooper and Rathert described a region (fig. 2) for which the sun was $\pm 20^\circ$ fore and aft relative to the wing and $\pm 45^\circ$ to the side from zenith (sun directly overhead), in which the shock shadowgraph was visible. Since the wings of their airplanes were unswept, the shock shadowgraph could be observed either looking towards the sun or looking away from the sun.

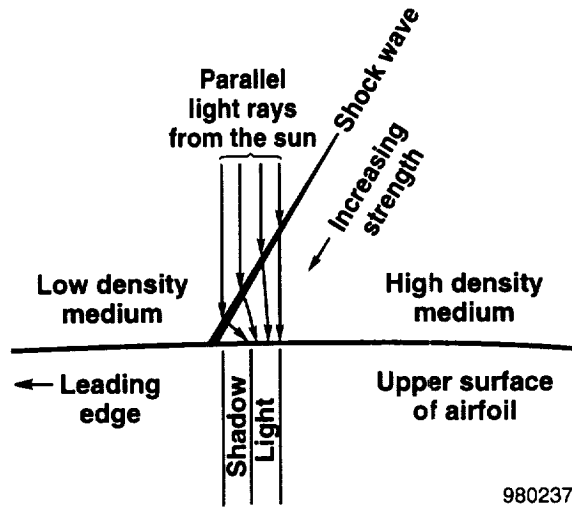


Figure 1. Schematic of shadowgraph physics.[1]

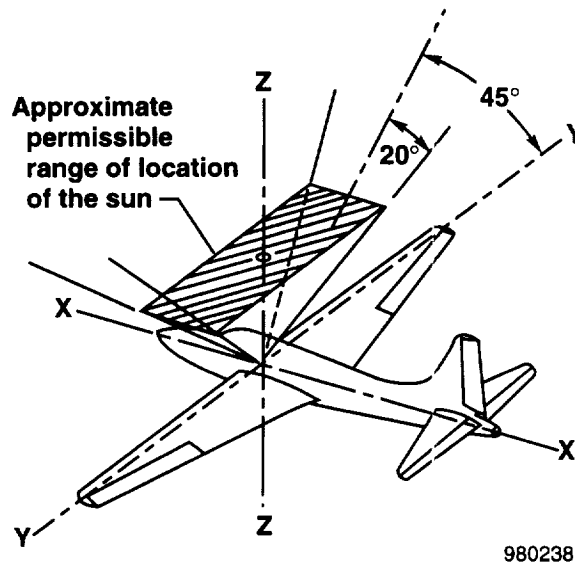


Figure 2. Proper orientation of the sun with respect to airplane axis, unswept wing.[1]

INSTRUMENTATION

The L-1011 aircraft was equipped with an instrumentation system that recorded aircraft state parameters such as Mach number, altitude, heading, roll angle, and pitch angle. An Ashtech Z-12 global positioning system (GPS) was used to record the time-based longitude, latitude, and altitude of the aircraft. On the first flight, August 10, 1997, time of day was hand recorded when the shadowgraph of the outboard wing shock was visible. On the second flight, January 22, 1998, professional-quality time-synchronized Beta video recordings were used to determine the time of day when the shadowgraph of the outboard wing shock was visible. Still photographs were taken on both flights.

TEST CONDITIONS

A limited number of observations of compression shock waves were taken on two flights with the Orbital Sciences Corporation's L-1011 aircraft flying between an altitude of 35,000 and 38,000 ft and at a nominal Mach number of 0.85 off the coast of Baja California, Mexico (fig. 3). The first flight was on August 10, 1997 and the second flight was on January 22, 1998. Data was taken approximately each hour by flying the aircraft in 360° or 540° turns banked at 20° to 30° and between 20° and 31.5° North latitude at approximately -119° East longitude. This experiment was flown piggyback with a primary experiment.

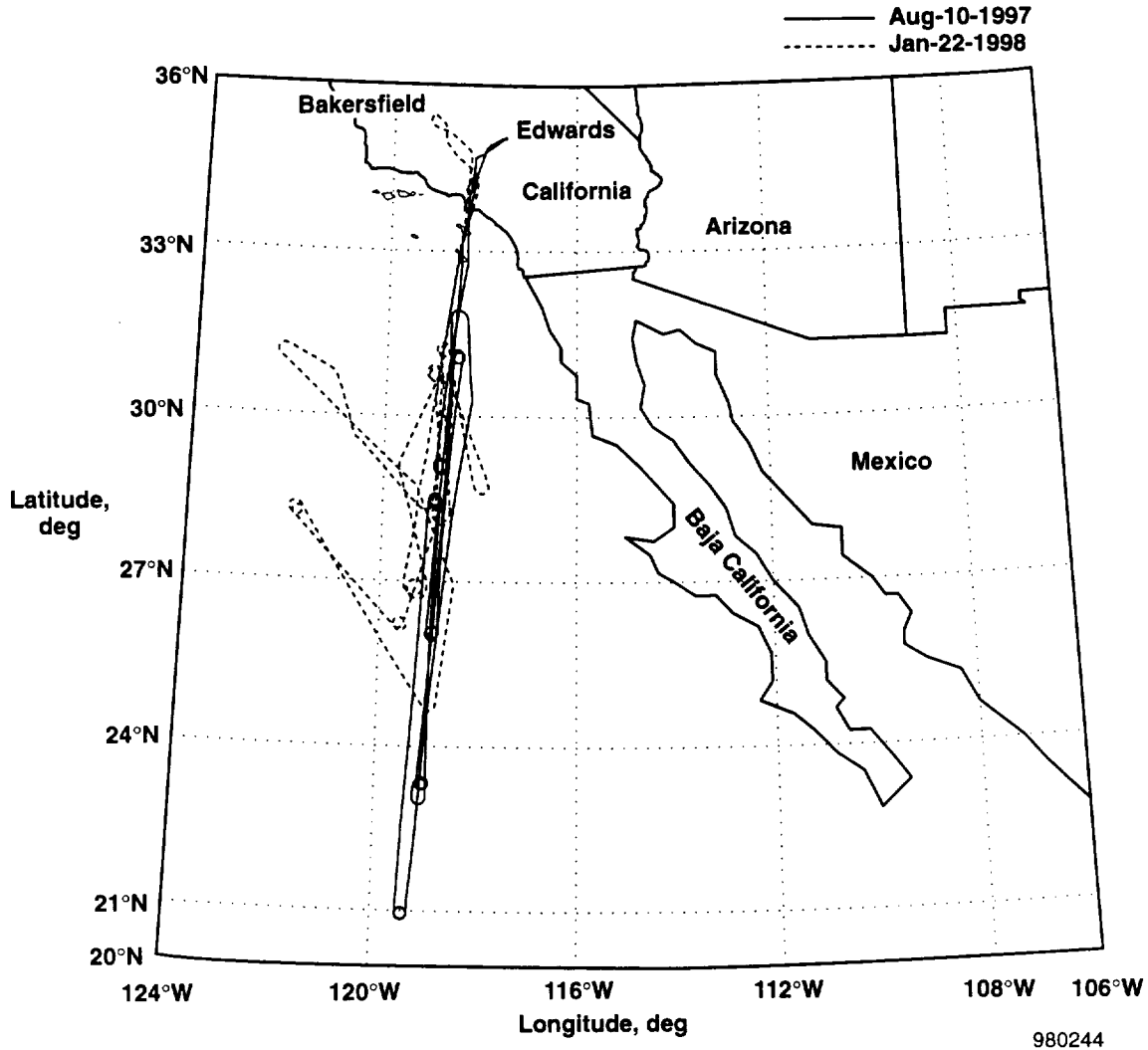


Figure 3. L-1011 flight tracks west of Baja California, Mexico.

DATA ANALYSIS

The following computations were performed to determine the orientation of the sun when the shadowgraphs were observed. First, the sun's elevation from the local horizon and azimuth were computed

from true north [6 and 7] using the flight date and time, and the aircraft latitude, longitude, and altitude as measured by the global positioning system. The elevation angle was corrected for atmospheric refraction [6 and 7] assuming a standard day temperature and measured ambient pressure at the altitude of the aircraft [8]. Second, the sun elevation and azimuth were converted into Cartesian distances north, east, and below the aircraft, assuming an arbitrary distance to the sun. (This distance drops out of the computations later, so its magnitude is not important.) Third, the north, east, and down components to the sun were rotated, first through the heading, then pitch, then roll of the aircraft. A final rotation of the components was made to align the quarter chordline axis with the wing of the aircraft being viewed, corresponding to the wing-sweep angle of 35° . For the right wing this angle is 125° and for the left wing it is 235° . Lastly, these component distances to the sun were converted to elevation above the wing and azimuth relative to the right wing quarter chordline, positive to the right, or clockwise. Reference 9 describes the equations and procedures to determine these angles.[9] The data obtained from the left wing was transposed to the right wing. In this way data from both wings could be compared, no matter what day, time, position, or attitude of the aircraft.

RESULTS

Figure 4 shows the shadowgraph from the wing compression shock looking towards the sun ($-90^\circ < \text{sun azimuth relative to quarter chordline} < +90^\circ$). As described previously in the Background section of this paper, the shadowgraph on the wing is noted by the dark band extending from inboard to outboard, with a light band immediately downstream of it. Figure 5 shows a similar view of the shock

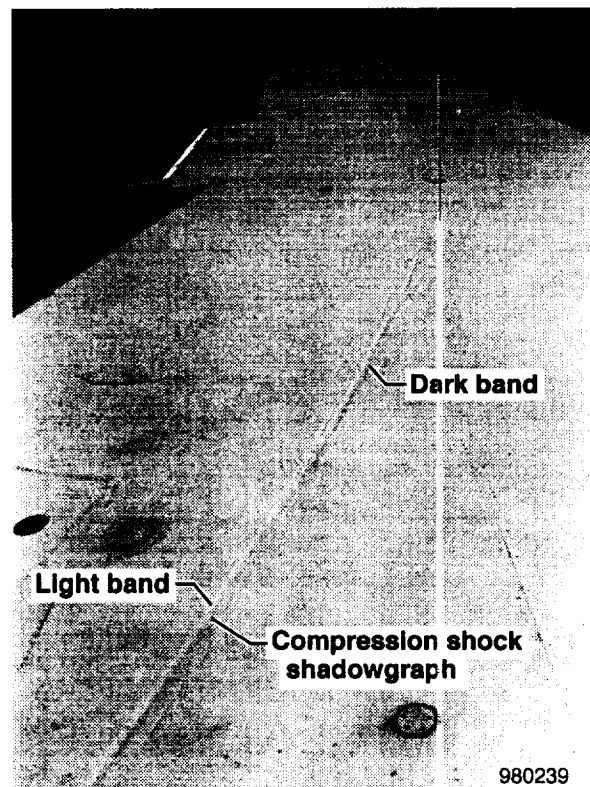


Figure 4. Wing compression shock shadowgraph looking towards sun.

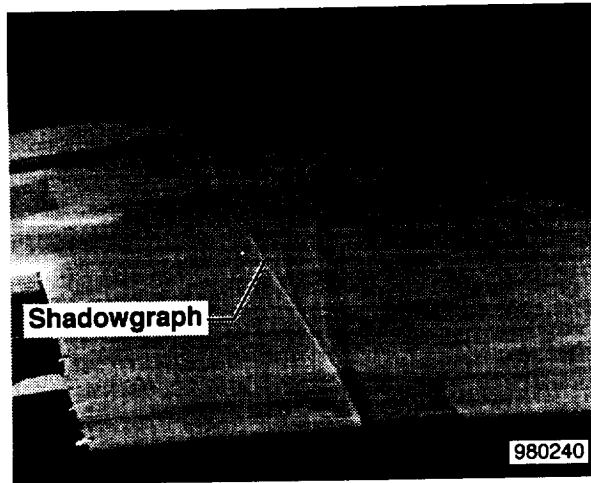


Figure 5. Wing compression shock shadowgraph looking away from sun.

shadowgraph looking away from the sun ($+90^\circ < \text{sun azimuth relative to quarter chordline} < +270^\circ$), in this case at a fairly low angle relative to the wing quarter chordline. The shock above the wing (fig. 4) is barely visible just outboard of the fuselage shadow and forward of the shock shadowgraph along the wing span. The shock can be seen more clearly with the proper background, as shown in figure 6, and appears here to be at the wingtip. The background that worked well in this case consisted of scattered alto-cumulus clouds with the blue ocean below. The wing shock appears to be approximately 6 ft (2 m) high.

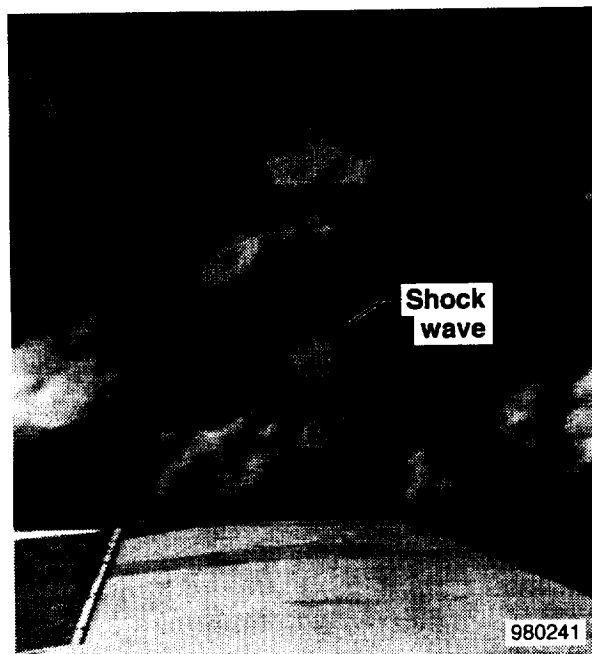
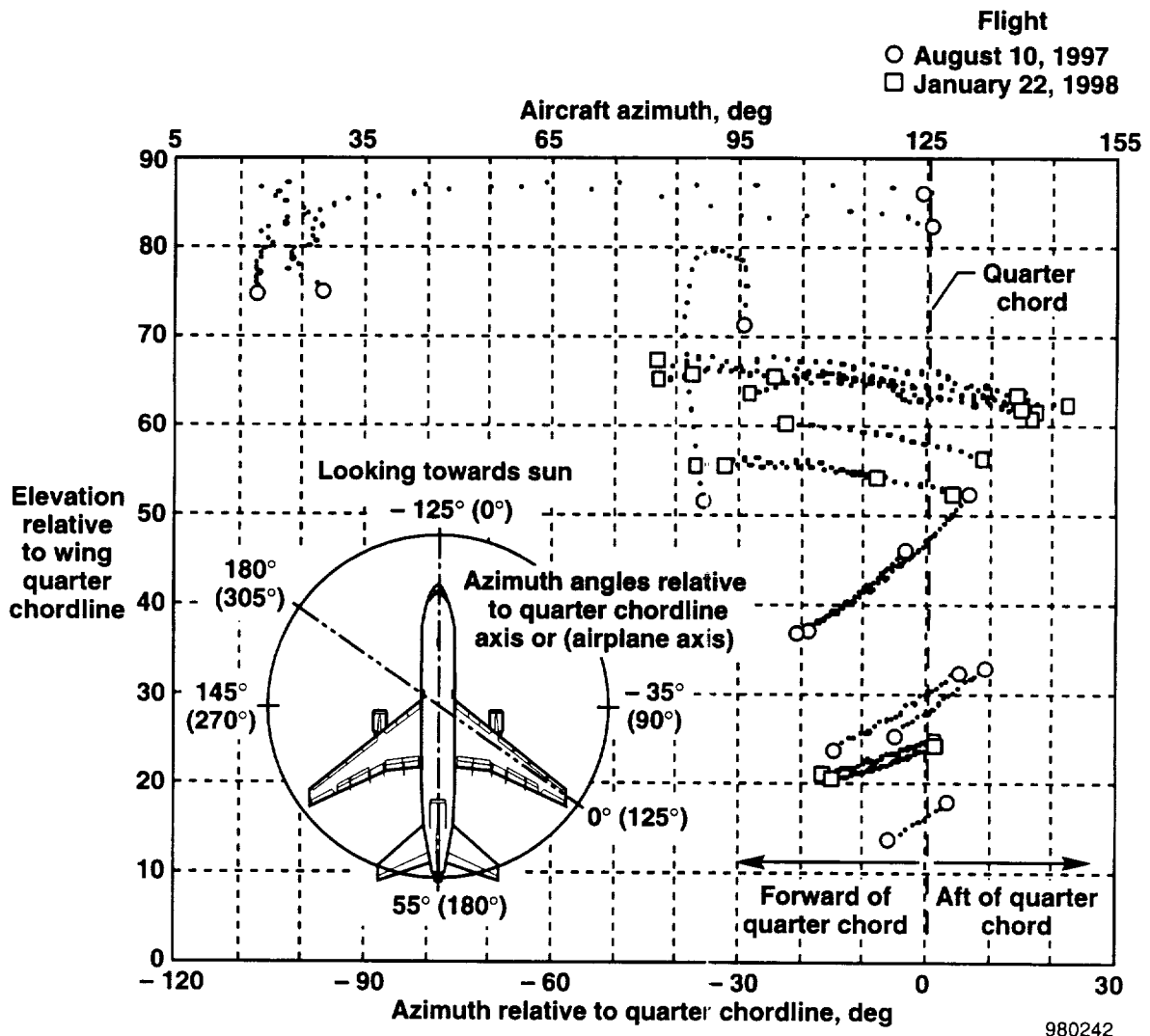


Figure 6. Photo of wingtip shock.

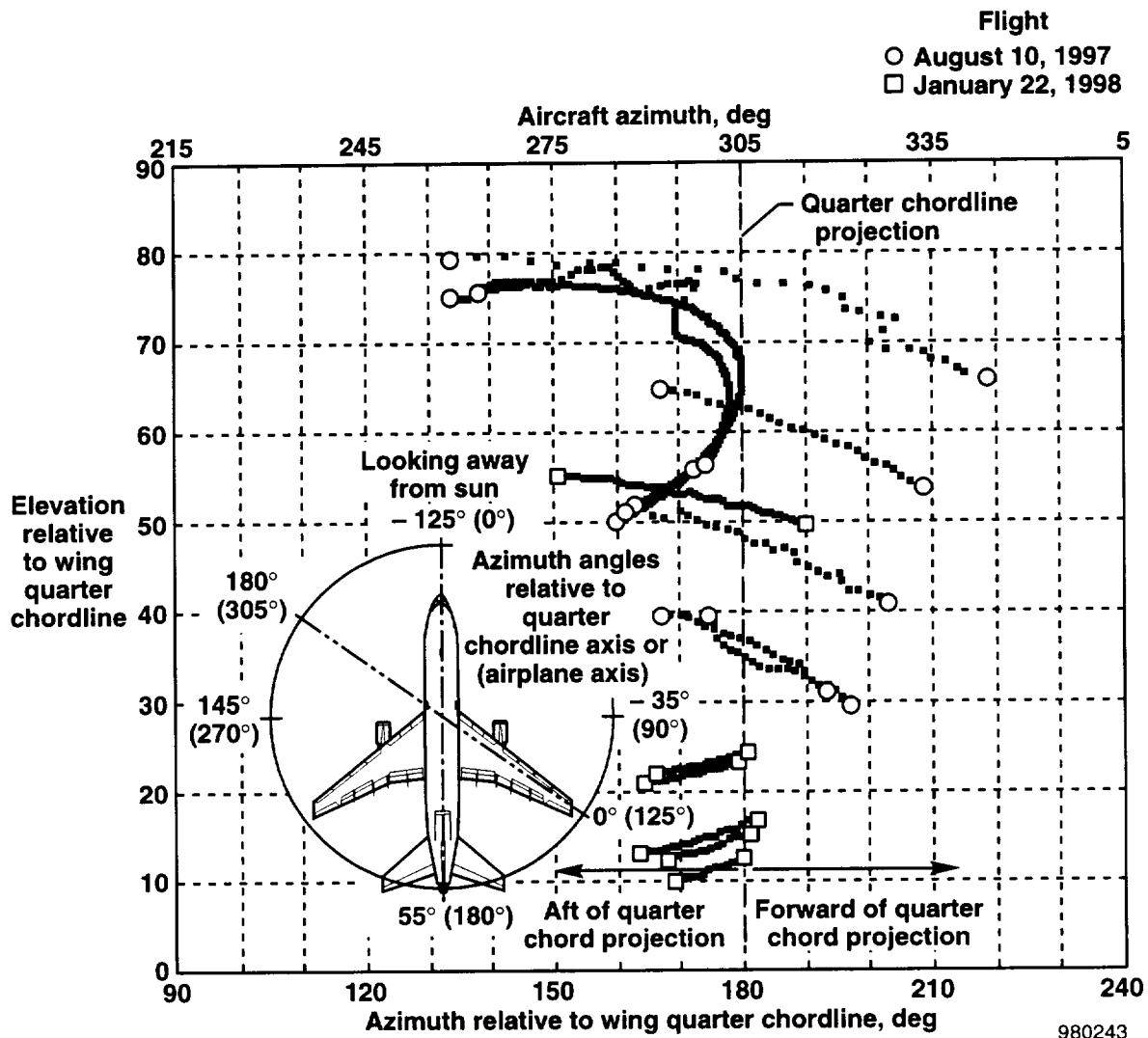
The test conditions for which the wing compression shock shadowgraph was visible looking towards the sun is shown in figure 7(a). A sketch of the planform of the L-1011 is included to help orient the reader. At low sun elevations relative to the wing, of 20° to 30° , the shadowgraph was visible only for a short period of time during the banked turns, for sun azimuths from 15° forward and 5° aft relative to the wing quarter chordline. At the low oblique sun elevations relative to the wing, the shadowgraph did not accurately portray the shock location. Instead, when looking towards the sun, it appeared that the shadowgraph was projecting the image of the shock near the wingtip inboard. When the sun is between 60° and 70° elevation relative to the wing, the shadowgraph is visible for a longer duration during the banked turn, for azimuths from approximately 40° forward to 20° aft of the quarter chordline. When the sun is 75° or higher, the shock was visible from approximately -100° to 0° relative to the quarter chordline. For best results bright sunlight on the aircraft is required and high sun angles relative to the wing are desired.



(a) Looking towards sun.

Figure 7. Required sun azimuth and elevation angles for viewing wing compression shock shadowgraph.

Test conditions looking away from the sun, and when the wing compression shock shadowgraph was visible, are shown in figure 7(b). Again for low sun elevation angles of 10° to 25° relative to the wing, the wing compression shock shadowgraph was visible only briefly during the banked turns, between sun azimuths approximately even with the quarter chordline projection to 15° aft of the quarter chordline projection. Between sun elevation angles of 65° to 80° , the duration increased greatly. At these sun elevations, the wing compression shock shadowgraph could be seen for sun azimuth angles of 35° forward to 45° aft of the quarter chordline projection.



(b) Looking away from sun.

Figure 7. Concluded.

The wing compression shock shadowgraphs were observed for sun elevations relative to the horizon of 12° to 76° in August and 25° to 42° in January. These sun elevation angles are not necessarily limits, but rather documented observations during piggyback flights. The technique requires a bright sun.

Cooper and Rathert noted that the technique was not as effective in the winter months, presumably near Moffett Field, California, at a latitude of approximately 37.4°.

CONCLUDING REMARKS

For two flights of an L-1011 aircraft, sun elevation and azimuth angles were documented for which wing compression shock shadowgraphs were visible relative to the wing quarter chordline. The data was taken during banked turns at a Mach number of 0.85 and an altitude of 35,000 ft (10,700 m). Photographs and videotape recording of the shadowgraphs were taken during the flights.

Bright sunlight on the aircraft is required and high sun angles relative to the wing are desired for best results.

Looking toward the sun, and at low sun elevations relative to the wing of 20° to 30°, the wing compression shock shadowgraph was visible only briefly during banked turns, for sun azimuths from 15° forward and 5° aft relative to the wing quarter chordline. When the sun is 75° or higher, the shock was visible from approximately -100° to 0° relative to the quarter chordline.

With the sun behind the observer, and for low sun elevation angles of 10° to 25° relative to the wing, the wing compression shock shadowgraph was visible only briefly during banked turns, between sun azimuths approximately even with the quarter chordline projection to 15° aft of the quarter chordline projection. Between sun elevation angles of 65° to 80°, the wing compression shock shadowgraph was visible for sun azimuth angles of 35° forward to 45° aft of the quarter chordline projection.

The shock wave at the wingtip can be observed on the low wing during a banked turn with the proper background, such as alto-cumulus clouds over a blue ocean.

*Dryden Flight Research Center
National Aeronautics and Space Administration
Edwards, California, May, 1998*

APPENDIX

The following procedure was used to determine the sun azimuth and elevation angles with respect to the wing quarter chordline for the flight on January 22, 1998. For years other than 1998, the constants in equations (1), (2), (3), (4), (5), and (8) could change. Check the Astronomical Almanac for the year of interest.

NOMENCLATURE

az	azimuth of sun from true north, deg
az_w	sun azimuth to right of wing quarter chordline, deg
d	day of year number for 1998
dd	sun distance down from aircraft toward earth, au
de	sun distance east from aircraft, au
dn	sun distance north from aircraft, au
dx	sun distance along aircraft wing quarter chordline, au
dy	sun distance left of aircraft wing quarter chordline, au
dz	sun distance below aircraft wing quarter chordline, au
el	elevation of sun above local horizon, deg
el_{ref}	correction of elevation from atmospheric refraction, deg
el_w	sun elevation above wing quarter chordline, deg
EOE	equation of equinox value for the particular day, sec
g	mean anomaly, deg
GAST	Greenwich apparant sidereal time, hr
GPS	global positioning system
h	local hour angle, deg
L	mean longitude of sun, corrected for aberration, deg
mbar	millibar, a unit of pressure measurement
n	number of days from the epoch J2000.0
P	ambient air pressure, mbar
t	UTC time in decimal hours, hr
T_∞	ambient air temperature, K
UTC	universal time coordinated
z_g	aircraft ellipsoid altitude, from GPS, ft
α	right ascension, deg

ϵ	obliquity of the ecliptic, deg
δ	declination, deg
λ_g	aircraft geodetic north latitude, from GPS, deg
θ	aircraft pitch, deg
θ_e	ecliptic longitude, deg
θ_g	aircraft east longitude, from GPS, deg
ϕ	aircraft roll, deg
ψ	aircraft heading, deg
ψ_w	wing azimuth angle quarter chordline, deg

Calculate the number of days from the epoch J2000.0 based on the day of year number for 1998 and the UTC time in decimal hours

$$n = -731.50 + d + \frac{t}{24} \quad (1)$$

Mean longitude of sun, corrected for aberration

$$L = 280.460 + 0.9856474n \quad (2)$$

Mean anomaly

$$g = 357.528 + 0.9856003n \quad (3)$$

Ecliptic longitude

$$\theta_e = L + 1.915 \sin(g) + 0.020 \sin(2g) \quad (4)$$

Obliquity of ecliptic

$$\epsilon = 23.439 - 4 \times 10^{-7} n \quad (5)$$

Right ascension (in the same quadrant as θ_e)

$$\alpha = \tan^{-1}(\cos(\epsilon) \tan(\theta_e)) \quad (6)$$

Declination

$$\delta = \sin^{-1}(\sin(\epsilon) \sin(\theta_e)) \quad (7)$$

Equations (1) to (7) have a precision of 0.01°, pp. C24 [7].

Greenwich apparant sidereal time, pp. B61 [7]

$$\text{GAST} = 6.6306380 + 0.06570982d + 1.00273791t + \frac{\text{EOE}}{3600} \quad (8)$$

where EOE is the equation of equinox value for the particular day, pp. B8-B15 [7]. Because this quantity is not readily calculated, a look-up table of the appropriate day's value is used.

The aircraft position, as determined from GPS, is in geodetic north latitude, λ_g , east longitude, θ_g , and ellipsoid altitude, z_g .

Local hour angle, pp. B61 [7]

$$h = \theta_g - \alpha + \frac{360GAST}{24} \quad (9)$$

Azimuth of sun from true north, pp. B61 [7]

$$az = \tan^{-1} \left[\frac{-\cos(\delta) \sin(h)}{\sin(\delta) \cos(\lambda_g) - \cos(\delta) \cos(h) \sin(\lambda_g)} \right] \quad (10)$$

The correction of elevation from atmospheric refraction needs to be determined. This was determined from the altitude of the aircraft measured by GPS, and assuming 1976 U.S. Standard Atmosphere [8] conditions for temperature. Measured ambient pressure was used. Because the GPS measures ellipsoidal altitude, z_g , subtract the geodetic separation to get geometric altitude above mean sea level needed for the Standard Atmosphere. The geodetic separation is usually determined by a look-up table, but for this experiment the constant value of -99.4 ft (at Edwards AFB) was used for all calculations.

For elevations greater than 15°, pp. B62 [7]

$$el_{ref} = \frac{0.00452P}{T_{\infty} \tan(el)} \quad (11)$$

and for elevations less than or equal to 15°, pp. B62) [7]

$$el_{ref} = \frac{P \left[0.1594 + 0.0196el + 0.00002el^2 \right]}{T_{\infty} \left[1 + 0.505el + 0.0845el^2 \right]} \quad (12)$$

Elevation of sun above local horizon, pp. B61 [7]

$$el = \sin^{-1} \left[\sin(\delta) \sin(\lambda_g) + \cos(\delta) \cos(h) \cos(\lambda_g) \right] - el_{ref} \quad (13)$$

Find the distance of the sun from the aircraft in orthogonal north, east, and down in astronomical units (unit distance). This distance is arbitrary, and drops out of the equation at the end

$$dn = \cos(az) \cos(el) \quad (14)$$

$$de = \sin(az) \sin(el) \quad (15)$$

$$dd = -\sin(el) \quad (16)$$

Rotate these distances through aircraft yaw angle, then aircraft pitch, then aircraft roll, and finally by wing azimuth angle. Note that no dihedral angle was accounted for, which is appropriate for this aircraft. This rotation is given in matrix form by

$$\begin{bmatrix} dx \\ dy \\ dz \end{bmatrix} = \begin{bmatrix} \cos(\Psi_w) & \sin(\Psi_w) & 0 \\ -\sin(\Psi_w) & \cos(\Psi_w) & 0 \\ 0 & 0 & 1 \end{bmatrix} \begin{bmatrix} 1 & 0 & 0 \\ 0 & \cos(\phi) & \sin(\phi) \\ 0 & -\sin(\phi) & \cos(\phi) \end{bmatrix} \begin{bmatrix} \cos(\theta) & 0 & -\sin(\theta) \\ 0 & 1 & 0 \\ \sin(\theta) & 0 & \cos(\theta) \end{bmatrix} \begin{bmatrix} dn \\ de \\ dd \end{bmatrix} \quad (17)$$

$$\begin{bmatrix} dx \\ dy \\ dz \end{bmatrix} = \begin{bmatrix} \cos(\Psi_w) & \sin(\Psi_w) & 0 \\ -\sin(\Psi_w) & \cos(\Psi_w) & 0 \\ 0 & 0 & 1 \end{bmatrix} \begin{bmatrix} 1 & 0 & 0 \\ 0 & \cos(\phi) & \sin(\phi) \\ 0 & -\sin(\phi) & \cos(\phi) \end{bmatrix} \begin{bmatrix} \cos(\theta)\cos(\psi) & \cos(\theta)\sin(\psi) & -\sin(\theta) \\ -\sin(\psi) & \cos(\psi) & 0 \\ \sin(\theta)\cos(\psi) & \sin(\theta)\sin(\psi) & \cos(\theta) \end{bmatrix} \begin{bmatrix} dn \\ de \\ dd \end{bmatrix} \quad (18)$$

$$\begin{bmatrix} dx \\ dy \\ dz \end{bmatrix} = \begin{bmatrix} \cos(\Psi_w) & \sin(\Psi_w) & 0 \\ -\sin(\Psi_w) & \cos(\Psi_w) & 0 \\ 0 & 0 & 1 \end{bmatrix} \begin{bmatrix} \cos(\theta)\cos(\psi) & \cos(\theta)\sin(\psi) & -\sin(\theta) \\ \sin(\phi)\sin(\theta)\cos(\psi) - \cos(\phi)\sin(\psi) & \sin(\phi)\sin(\theta)\sin(\psi) + \cos(\phi)\cos(\psi) & \sin(\phi)\cos(\theta) \\ \cos(\phi)\sin(\theta)\cos(\psi) + \sin(\phi)\sin(\psi) & \cos(\phi)\sin(\theta)\sin(\psi) - \sin(\phi)\cos(\psi) & \cos(\phi)\cos(\theta) \end{bmatrix} \begin{bmatrix} dn \\ de \\ dd \end{bmatrix} \quad (19)$$

Multiplying this out gives the following three algebraic equations for dx , dy , and dz , respectively:

$$\begin{aligned} dx &= \left[\cos(\Psi_w)\cos(\theta)\cos(\psi) + \sin(\Psi_w)\{\sin(\phi)\sin(\theta)\cos(\psi) - \cos(\phi)\sin(\psi)\} \right] dn \\ &+ \left[\cos(\Psi_w)\cos(\theta)\sin(\psi) + \sin(\Psi_w)\{\sin(\phi)\sin(\theta)\sin(\psi) + \cos(\phi)\cos(\psi)\} \right] de \\ &+ \left[-\cos(\Psi_w)\sin(\theta) + \sin(\Psi_w)\sin(\phi)\cos(\theta) \right] dd \end{aligned} \quad (20)$$

$$\begin{aligned}
dy = & \left[-\sin(\Psi_w) \cos(\theta) \cos(\psi) + \cos(\Psi_w) \{ \sin(\phi) \sin(\theta) \cos(\psi) - \cos(\phi) \sin(\psi) \} \right] dn & (21) \\
& + \left[-\sin(\Psi_w) \cos(\theta) \sin(\psi) + \cos(\Psi_w) \{ \sin(\phi) \sin(\theta) \sin(\psi) + \cos(\phi) \cos(\psi) \} \right] de \\
& + \left[\sin(\Psi_w) \sin(\theta) + \cos(\Psi_w) \sin(\phi) \cos(\theta) \right] dd
\end{aligned}$$

$$\begin{aligned}
dz = & \left[\cos(\phi) \sin(\theta) \cos(\psi) + \sin(\phi) \sin(\psi) \right] dn & (22) \\
& + \left[\cos(\phi) \sin(\theta) \sin(\psi) - \sin(\phi) \cos(\psi) \right] de + \left[\cos(\phi) \cos(\theta) \right] dd
\end{aligned}$$

Now these components can be transformed into azimuth and elevation relative to the wing quarter chordline.

$$az_w = \tan^{-1} \left(\frac{dy}{dx} \right) \quad (23)$$

$$el_w = \tan^{-1} \left(\frac{-dz}{\sqrt{dx^2 + dy^2}} \right) \quad (24)$$

REFERENCES

1. Cooper, George E. and Rathert, George A.: *Visual observations of the shock wave in flight*. NACA RM A8C25, 1948.
2. Merzkirch, W.: *Techniques of flow visualization*. AGARD-AG-302, 1987.
3. Larmore, Lewis and Hall, Freeman F., Jr.: "Optics for the airborne observer." SPIE Journal, Vol. 9, No. 3, pp. 87–94, February–March 1971.
4. Crowder, James R.: *Flow visualization techniques applied to full-scale vehicles*. AIAA Atmospheric Flight Mechanics Conference, Monterey, California, AIAA-87-2421, pp. 164–171, August 1987.
5. Merzkirch, Wolfgang: *Flow Visualization*, Second Edition, Academic Press, Inc., Harcourt, Brace, Jovanovich, Publishers, 1987.
6. Nautical Almanac Office, United States Naval Observatory, and Her Majesty's Nautical Almanac Office, Royal Greenwich Observatory, *The Astronomical Almanac for the Year 1997*, U.S. Government Printing Office, Washington, D.C., 1995.
7. United States Naval Observatory, Nautical Almanac Office, and Her Majesty's Nautical Almanac Office, Royal Greenwich Observatory, *The Astronomical Almanac for the Year 1998*, U. S. Government Printing Office, Washington, D. C., 1996.
8. National Oceanic and Atmospheric Administration, National Aeronautics and Space Administration, United States Air Force, *U.S. Standard Atmosphere*, 1976, U. S. Government Printing Office, Washington, D. C., October 1976.
9. Fisher, David F., Haering, Edward A., Jr., Noffz, Gregory K., and Aguilar, Juan I.: *Determination of sun angles for observations of shock waves on a transport aircraft*. NASA/TM-1998-206551, 1998. Also at <http://www.dfrc.nasa.gov/DTRS/1998/index.html>.

REPORT DOCUMENTATION PAGE

Form Approved
OMB No. 0704-0188

Public reporting burden for this collection of information is estimated to average 1 hour per response, including the time for reviewing instructions, searching existing data sources, gathering and maintaining the data needed, and completing and reviewing the collection of information. Send comments regarding this burden estimate or any other aspect of this collection of information, including suggestions for reducing this burden, to Washington Headquarters Services, Directorate for Information Operations and Reports, 1215 Jefferson Davis Highway, Suite 1204, Arlington, VA 22202-4302, and to the Office of Management and Budget, Paperwork Reduction Project (0704-0188), Washington, DC 20503.

1. AGENCY USE ONLY (Leave blank)		2. REPORT DATE September 1998	3. REPORT TYPE AND DATES COVERED Technical Memorandum	
4. TITLE AND SUBTITLE Determination of Sun Angles for Observations of Shock Waves on a Transport Aircraft			5. FUNDING NUMBERS WU 529 59 04 00 RR 00 000	
6. AUTHOR(S) David F. Fisher, Edward A. Haering, Jr., Gregory K. Noffz, and Juan I. Aguilar				
7. PERFORMING ORGANIZATION NAME(S) AND ADDRESS(ES) NASA Dryden Flight Research Center P.O. Box 273 Edwards, California 93523-0273			8. PERFORMING ORGANIZATION REPORT NUMBER H-2251	
9. SPONSORING/MONITORING AGENCY NAME(S) AND ADDRESS(ES) National Aeronautics and Space Administration Washington, DC 20546-0001			10. SPONSORING/MONITORING AGENCY REPORT NUMBER NASA/TM-1998-206551	
11. SUPPLEMENTARY NOTES Extended version of a conference paper presented at the 8th International Symposium on Flow Visualization, Sorrento, Italy, Sept. 1-4, 1998				
12a. DISTRIBUTION/AVAILABILITY STATEMENT Unclassified—Unlimited Subject Category 02			12b. DISTRIBUTION CODE	
13. ABSTRACT (Maximum 200 words) Wing compression shock shadowgraphs were observed on two flights during banked turns of an L-1011 aircraft at a Mach number of 0.85 and an altitude of 35,000 ft (10,700 m). Photos and video recording of the shadowgraphs were taken during the flights to document the shadowgraphs. Bright sunlight on the aircraft was required. The time of day, aircraft position, speed and attitudes were recorded to determine the sun azimuth and elevation relative to the wing quarter chordline when the shadowgraphs were visible. Sun elevation and azimuth angles were documented for which the wing compression shock shadowgraphs were visible. The shadowgraph was observed for high to low elevation angles relative to the wing, but for best results high sun angles relative to the wing are desired. The procedures and equations to determine the sun azimuth and elevation angle with respect to the quarter chordline is included in the Appendix.				
14. SUBJECT TERMS Flight test, Flow visualization, GPS, L-1011 aircraft, Shadowgraph, Shock waves			15. NUMBER OF PAGES 20	
			16. PRICE CODE A03	
17. SECURITY CLASSIFICATION OF REPORT Unclassified	18. SECURITY CLASSIFICATION OF THIS PAGE Unclassified	19. SECURITY CLASSIFICATION OF ABSTRACT Unclassified	20. LIMITATION OF ABSTRACT Unlimited	